Journal of Alloys and Compounds 509 (2011) 134–140

Contents lists available at ScienceDirect

Journal of Alloys and Compounds

journal homepage: www.elsevier.com/locate/jallcom

Synthesis of lanthanum carbonate nanoparticles via sonochemical method for preparation of lanthanum hydroxide and lanthanum oxide nanoparticles

Masoud Salavati-Niasari[a,b,*], Ghader Hosseinzadeh[a], Fatemeh Davar[a]

[a] Institute of Nano Science and Nano Technology, University of Kashan, Kashan, P.O. Box 87317-51167, Islamic Republic of Iran
[b] Department of Inorganic Chemistry, Faculty of Chemistry, University of Kashan, Kashan, P.O. Box 87317-51167, Islamic Republic of Iran

ARTICLE INFO

Article history:
Received 23 June 2010
Received in revised form 31 August 2010
Accepted 2 September 2010
Available online 15 September 2010

Keywords:
$La_2(CO_3)_3$
Ultrasonic
Nanoparticles
La_2O_3

ABSTRACT

Lanthanum carbonate nanoparticles were synthesized from the reaction of lanthanum acetate and Na_2CO_3 under sonication via sonochemical method. Lanthanum hydroxide nanoparticles were prepared by facial hydrothermal processing from the resulted product at 110 °C for 24 h. The role of surfactant, calcination temperature and sonication time were investigated on the morphology and particle size of the products. Products were characterized by X-ray diffraction (XRD), scanning electron microscopy (SEM), transmission electron microscopy (TEM), X-ray photoelectron spectrum (XPS), and Fourier transform infrared (FT-IR) spectra. La_2O_3 nanoparticles were obtained by calcinations of the nanoparticles of lanthanum carbonate at 600 °C.

1. Introduction

Considerable attention has recently been attracted towards the fabrication of nano materials because of large differences found in their properties when the particles size is reduced, and therefore new technological application can arise. Nanocrystalline materials have properties that otherwise unachievable with equilibrium materials [1–5]. Properties of this material depend strongly on their size and morphology thus the synthesis of nanostructures with different size and morphology is very important [6–8]. Among rare earth compounds, lanthanum with have diverse industrial and technological application have been extensively used in many fields such as time resolved fluorescence labels for detection of biological warfare agents [10,9], dielectric materials in CMOS [11], catalyst [12], exhaust gas convertors [13], electrode materials [14], ceramic [15], hydrogen production for fuel cell [16], sensor [17], and other functional materials. So the study of lanthanum compound has been of great interest and there are many preparation methods for synthesis of these materials including: hydrothermal [18], sol-solvothermal [19], sol–gel [20], reveres micelles or micro emulsion [21], laser ablation [22], deposition methods [23] and so on. But some of these methods require more and expensive chemicals, longtime, high temperatures or pressure and expensive tools. In view of these problems we tried to synthesis lanthanum oxide by novel sonochemical method.

Among the many synthetic techniques available, the sonochemical method was shown to be a versatile technique for the preparation of complicated structures with different morphologies, such as nanorods [24], core–shell nanorods [25], nanospindles [26], and dendritic structures [27] as well as this method does not require high temperature or pressure. The ultrasound irradiation of the liquids induces acoustic cavitation, which means the formation, growth and implosive collapse of bubbles (cavitations' phenomenon). These bubbles generate a localized hotspot, which has the extreme high temperatures (45000 K), pressures (420 MPa), and cooling rates (10^{10} K s^{-1}) during acoustic cavitation and these produce the desired nanostructures [28,29]. The use of ultrasound radiation during the homogeneous precipitation of the precursor is expected to reduce the precipitation time of the precursor and to ensure the homogeneity of resulted products.

In this paper, we demonstrated that lanthanum carbonate nanoparticles could be successfully prepared by a simple sonochemical method from lanthanum acetate, $La(OAC)_3$, and sodium carbonate in an ultrasonic device. And so, we report a simple method for prepare of $La(OH)_3$ nanoparticles by facile hydrothermal processing from lanthanum carbonate nanoparticles at the presence of hydrazine. La_2O_3 nanoparticles with average size about 30 nm were prepared by calcinations of the as-prepared products at 600 °C. In addition, the effects of some parameter on the formation of lanthanum hydroxide and lanthanum oxide (La_2O_3) nanoparticle were investigated. We believe that this manuscript will bring

* Corresponding author at: Institute of Nano Science and Nano Technology, University of Kashan, Kashan, P.O. Box 87317-51167, Islamic Republic of Iran.
Tel.: +98 361 5555 333; fax: +98 361 555 2 930.
E-mail address: salavati@kashanu.ac.ir (M. Salavati-Niasari).

0925-8388/$ – see front matter © 2010 Elsevier B.V. All rights reserved.
doi:10.1016/j.jallcom.2010.09.006

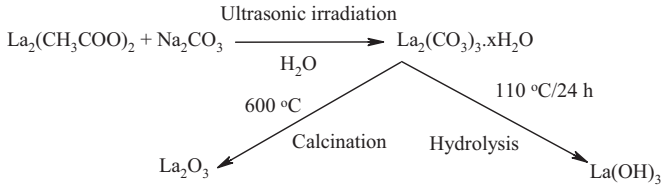

Scheme 1. Materials produced and formation methods of $La(OH)_3$ and La_2O_3 nanoparticles.

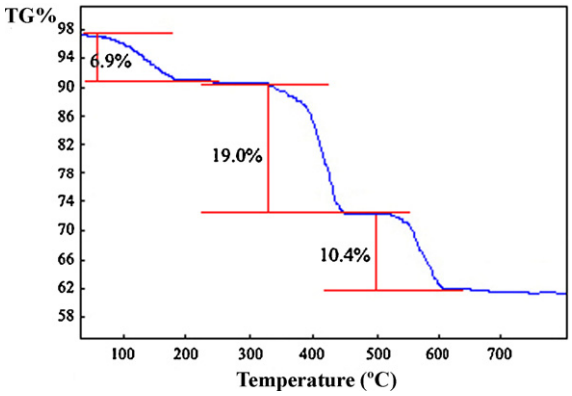

Fig. 1. Thermogravimetric pattern of the lanthanum carbonate (sample no. 2).

a novel strategy to synthesis of lanthanum carbonate, lanthanum oxide and lanthanum hydroxide nanoparticles.

2. Experimental

2.1. Materials and physical measurements

All the chemicals reagents used in our experiments were of analytical grade and were used as received without further purification. A multiwave ultrasonic generator (Sonicator 3000; Bandeline, MS 72, Germany), equipped with a converter/transducer and titanium oscillator (horn), 12.5 mm in diameter, operating at 20 kHz with a maximum power output of 60 W, was used for the ultrasonic irradiation. The ultrasonic generator automatically adjusted the power level. The wave amplitude in each experiment was adjusted as needed. XRD patterns were recorded by a Rigaku D-max C III, X-ray diffractometer using Ni-filtered Cu Kα radiation. Elemental analyses were obtained from Carlo ERBA Model EA 1108 analyzer. Thermogravimetric-differential thermal analysis (TG-DTA) were carried out using a thermal gravimetric analysis instrument (Shimadzu TGA-50H) with a flow rate of 20.0 mL min^{-1} and a heating rate of 10 °C min^{-1} in the inert atmosphere. X-ray Photoelectron Spectroscopy (XPS) of the as-prepared products were measured on an ESCA-3000 electron spectrometer with nonmonochromatized Mg Kα X-ray as the excitation source. Scanning electron microscopy (SEM) images were obtained on Philips XL-30ESEM equipped with an energy dispersive X-ray spectroscopy. Transmission electron microscopy (TEM) images were obtained on a Philips EM208 transmission electron microscope with an accelerating voltage of 100 kV. Fourier transform infrared (FT-IR) spectra were recorded on Shimadzu Varian 4300 spectrophotometer in KBr pellets.

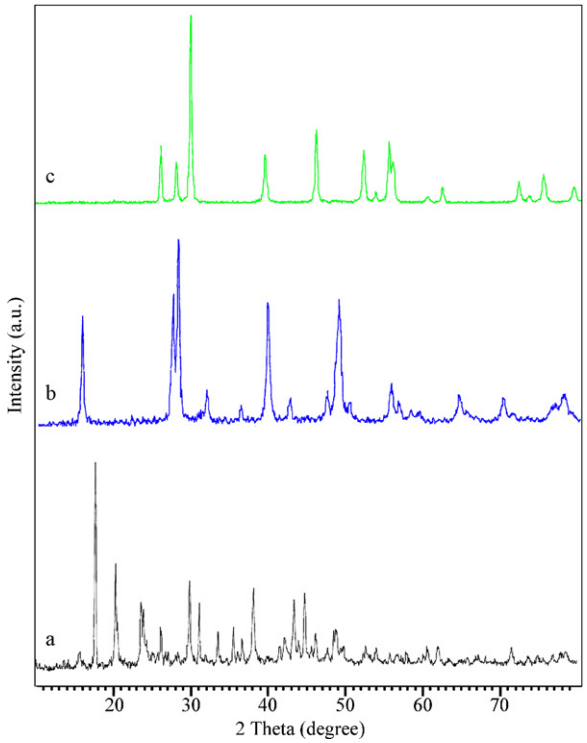

Fig. 2. XRD patterns of (a) sample no. 2, (b) sample no. 5 and (c) sample no. 7.

2.2. Preparation of $La_2(CO_3)_3 \cdot xH_2O$ nanoparticles

To prepare lanthanum carbonate nanoparticles solution of Na_2CO_3, 0.8 g in 30 ml (0.251 M) water were added dropwise to 0.8 g solution of $La(OAC)_3$ (lanthanum acetate) (0.051 M) in 50 ml water. Then the suspension was ultrasonically irradiated in different times with a high density ultrasonic probe immersed directly in to the solution. The white resulted products were collected by centrifugation 6000 rpm and washed three times with distilled water and dried in oven at 50 °C.

2.3. Preparation of $La(OH)_3$ nanoparticles

In a typical synthesis, 0.4 g of the obtained $La_2(CO_3)_3$ nanoparticles and a solution of N_2H_4 (1 mmol) in 5 ml of water was added to 15 ml of H_2O and then the mixture was transferred into a Teflon-lined stainless steel autoclave of 30 ml capacity. The autoclave was maintained at 110 °C for 24 h and then was allowed to cool to room temperature. Subsequently, the resultant white solid product was centrifuged, washed with distilled water and ethanol to remove the ions possibly remaining in the final product and finally dried at 60 °C in air.

2.4. Preparation of La_2O_3 nanoparticles

The obtained lanthanum carbonate nanoparticle was calcinated at 600 °C for 2 h in order to synthesize lanthanum oxide nanoparticles (Scheme 1). Effects of some other parameters such as time of sonication, calcinations temperature and surfac-

Table 1
Experimental condition for the preparation of $La_2(CO_3)_3$, $La(OH)_3$ and La_2O_3.

Sample no.	Na_2CO_3 (g)	$La(OAC)_3$ (g)	Time of sonication (min)	Temperature of calcination	Time and temperature of hydrothermal
1	0.8	0.8	15	–	–
2	0.8	0.8	30	–	–
3	0.8	0.8	45	–	–
4	0.8	0.8	60	–	–
5	0.8	0.8	30	–	24 h (110 °C)
6	0.8	0.8	30	400 °C for 2 h	–
7	0.8	0.8	30	600 °C for 2 h	–
8	0.8	0.8	30	650 °C for 2 h	–
9	0.8	0.8	30	700 °C for 2 h	–
10	0.8	0.8	30	750 °C for 2 h	–
11	0.8	0.8	30	800 °C for 2 h	–
12	0.8	0.8 + 3 ml PEG	30	–	–
13	0.8	0.8	–	–	–

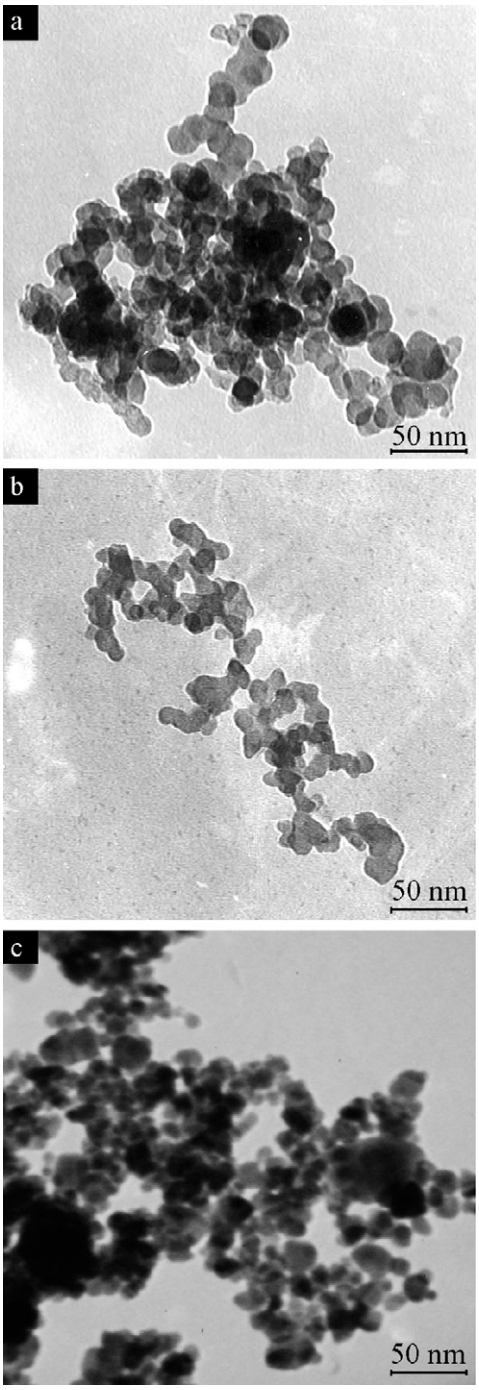

Fig. 3. TEM images of (a) sample no. 2, (b) sample no. 5 and (c) sample no. 7.

tants were investigated according to Table 1. Pay attention that 3 mL polyethylene glycol (PEG) 600 as surfactant was added to lanthanum acetate solution.

3. Results and discussion

Fig. 1 shows the TGA curve of the as-prepared carbonate, sample no. 2, in nitrogen atmosphere from ambient temperature to 800 °C. The lanthanum carbonate nanoparticles showed three steps Fig. 1: at ca. 125 °C (weight loss ~ 6.9%), at ca. 480 °C (weight loss ~ 19.0%) and at ca. 590 °C (weight loss ~ 10.4%) with an overall weight loss of 36.3% [30], which is due to the evaporation of H_2O molecules in the $La_2(CO_3)_3{\cdot}1.7H_2O$, and then evolution of CO_2 during the thermal decomposition. The individual experimental weight losses in the

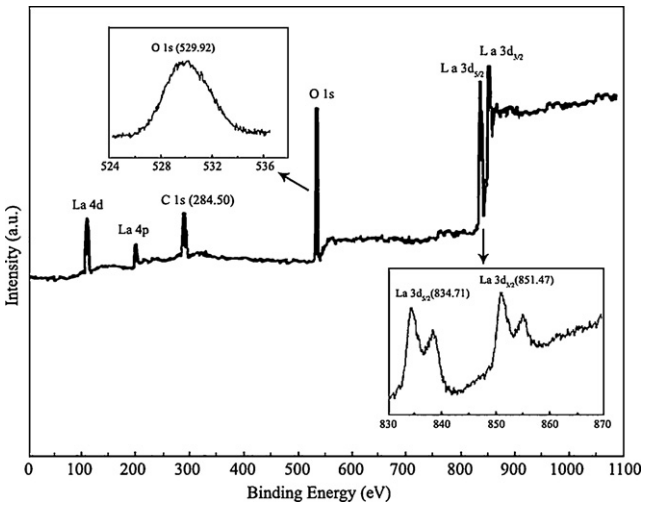

Fig. 4. XPS spectra of the La_2O_3 (sample no. 7): survey spectrum; La 3d region and O 1s region.

TGA pattern, corresponding to formation of the dehydrated carbonate, $La_2(CO_3)_3$, the dioxycarbonate, $La_2O_2CO_3$, and the oxide, La_2O_3, agree well with the calculated weight losses (7.4, 19.2 and 11.9 mass%, respectively). Studies on the thermal behavior of the as-prepared carbonate, sample no. 2, showed features similar to those observed for other lanthanum carbonates such as $La_2(CO_3)_3{\cdot}8H_2O$, $La_2(CO_3)_3{\cdot}1.4H_2O$, $La_2(CO_3)_2(OH)_2{\cdot}H_2O$, $La_2(CO_3)_3$, etc [30]. The above-mentioned carbonates decompose to La_2O_3 through the intermediate, $La_2O_2CO_3$, as in the present study. So, the following pattern is proposed for decomposition sample no. 2:

$$La_2(CO_3)_3 \cdot 1.7H_2O \overset{125\,^{\circ}C}{\longrightarrow} La_2(CO_3) \overset{480\,^{\circ}C}{\longrightarrow} La_2O_2CO_3 \overset{590\,^{\circ}C}{\longrightarrow} La_2O_3$$

Shown in Fig. 2a is the wide-angle XRD pattern of sample no. 2, $La_2(CO_3)_3{\cdot}xH_2O$. All of the diffraction peaks can be indexed to the

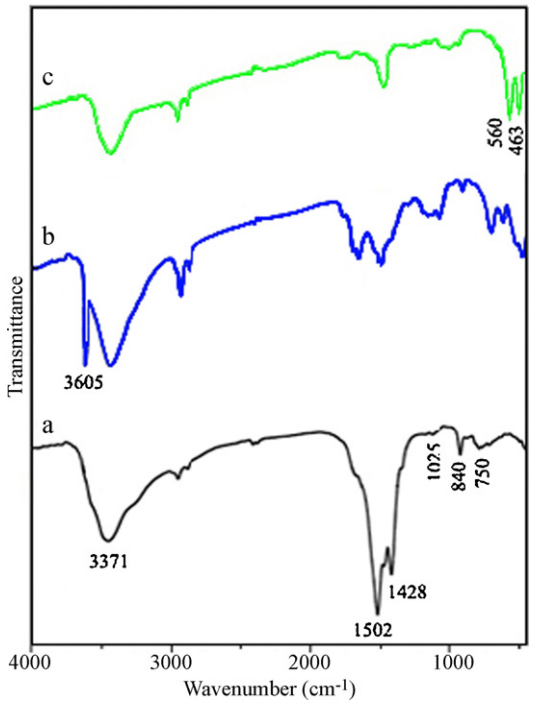

Fig. 5. FT-IR spectra of the as-synthesized products: (a) sample no. 2, (b) sample no. 5, and (c) sample no. 7.

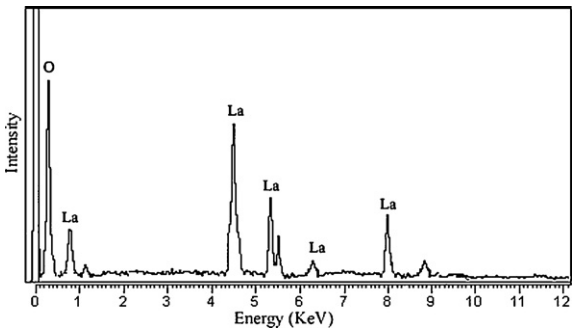

Fig. 6. EDS patterns of $La(OH)_3$ (sample no. 5), nanoparticles.

orthorhombic type of $La_2(CO_3)_3$ with lattice constants $a = 8.990$ Å and $c = 9.675$ Å, consistent with the values of standard card JCPDS No. 28-0512. Fig. 2b confirmed hexagonal phase of lanthanum hydroxide, sample no. 5, with high purity (space group P63/m, with $a = 6.547$ Å, $b = 6.547$ Å and $c = 3.854$ Å, JCPDS No.83-2034). The broadening of the peaks indicated that the particles were of nanometer scale. From XRD data (Fig. 2b), the crystallite size (D_c) of the as-prepared $La(OH)_3$ was calculated to be 19 nm using the Scherrer equation:

$$D_c = \frac{K\lambda}{\beta \cos\theta} \quad (1)$$

where β is the breadth of the observed diffraction line at its half-intensity maximum, K is the so-called shape factor, which usually takes a value of about 0.9, and λ is the wavelength of X-ray source used in XRD [31]. The XRD pattern of the sample no. 7 is shown in Fig. 2c. All diffraction peaks can be indexed as the cubic La_2O_3 with lattice constant $a = 11.347$ Å which is very consistent with the values in the standard card (JCPDS 22-369). The average particle size is found to be 30 nm.

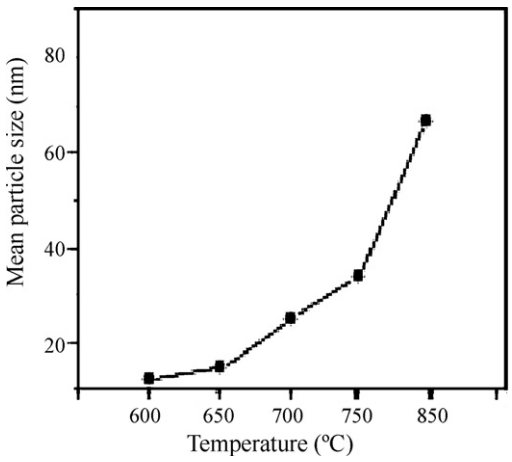

Fig. 7. The mean particle size of La_2O_3 nanoparticles as a function of calcination temperature.

TEM photograph of the products have been given in Fig. 3. Fig. 3a–c shows TEM images of $La_2(CO_3)_3$ (sample no. 2), $La(OH)_3$ (sample no.5) and La_2O_3 (sample no. 7) nanoparticles, respectively. The size of $La_2(CO_3)_3$ nanoparticles obtained from the XRD diffraction patterns are in close agreement with the TEM studies which shows sizes of 25–35 nm for sample no.2 with quasi spherical shapes, also the particles are observed to be agglomerated (Fig. 3a). Fig. 3b shows TEM image of $La(OH)_3$ nanoparticles, sample no. 5. The particle size of $La(OH)_3$ was about 16–20 nm. According to the TEM image of La_2O_3 nanoparticles, sample no. 7, the La_2O_3 particle is about 30 nm in size with spherical in shape Fig. 3c.

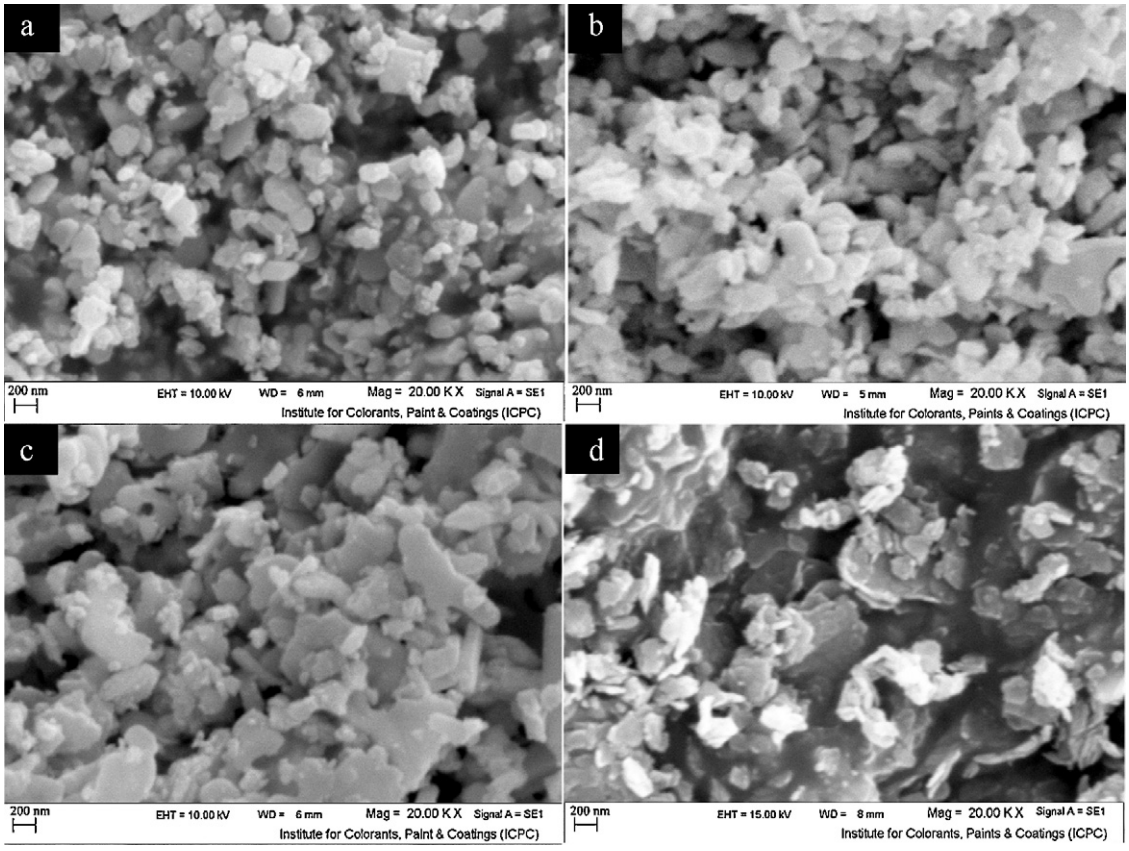

Fig. 8. SEM images of the La_2O_3 nanoparticles: (a) sample no. 8, (b) sample no. 9, (c) sample no. 10, and (d) sample no. 11.

Further evidence for the composition was illuminated by the XPS of the La_2O_3 (sample no. 7). The binding energies obtained in the XPS analysis were corrected for specimen by referencing the C 1s to 284.50 eV. The survey XPS spectrum of the product (Fig. 4) suggests that there are no other metal elements on the surface of the sample except for La. Fig. 4 shows that the binding energy of La $3d_{5/2}$ and La $3d_{3/2}$ are 834.71 and 851.47 eV, respectively [32,33]. In Fig. 4, it can be seen that the O 1s profile is asymmetric, indicating that two oxygen species are present in the nearby region. The peak at about 529.92 eV can be indexed to the O^{2-} in the La_2O_3

FT-IR spectra were recorded to show the chemical groups for every product at each step of the synthesis. The infrared spectra of sample no. 2, sample no. 5 and sample no. 7 are shown in Fig. 5. The absorption peak at 3371 cm^{-1} in Fig. 5a is attributed to the stretching vibration of the O–H bond and the bending vibration of H–O–H from water molecules on the external surface of the samples during handling to record the spectra [34–38]. The absorption bands at 1502 cm^{-1} and 1428 are attributed to the υ_3 mode of CO_3^{2-} group. The splitting of the band could be due to the carbonate ions located at a crystallographically non-equivalent site [39]. The absorption bands at 1025, 840, and 750 cm^{-1} are assigned to the υ_1, υ_2, and υ_4 modes of the carbonate ion, respectively [30,40,41]. According to Fig. 5b a sharp peak was appeared at 3605 cm^{-1} which is assigned for stretching mode of OH^- in $La(OH)_3$ (sample no. 5). The dehydration of the $La(OH)_3$ at 600 °C results in the formation of the final product La_2O_3 nanostructures, sample no. 7, as described in reaction (2). In Fig. 5c the absorption band of carbonate ions were reduced and the absorption band of cubic phase La_2O_3 appears at 560 cm^{-1} and 463 cm^{-1}. This is in agreement with the corresponding XRD spectrum where reflections for lanthanum oxide and weak reflections of lanthanum oxide carbonate were observed together. In this temperature there were no additional peaks observed in the corresponding XRD spectrum except cubic La_2O_3. So pure lanthanum oxide can be obtained by calcination of the precipi-

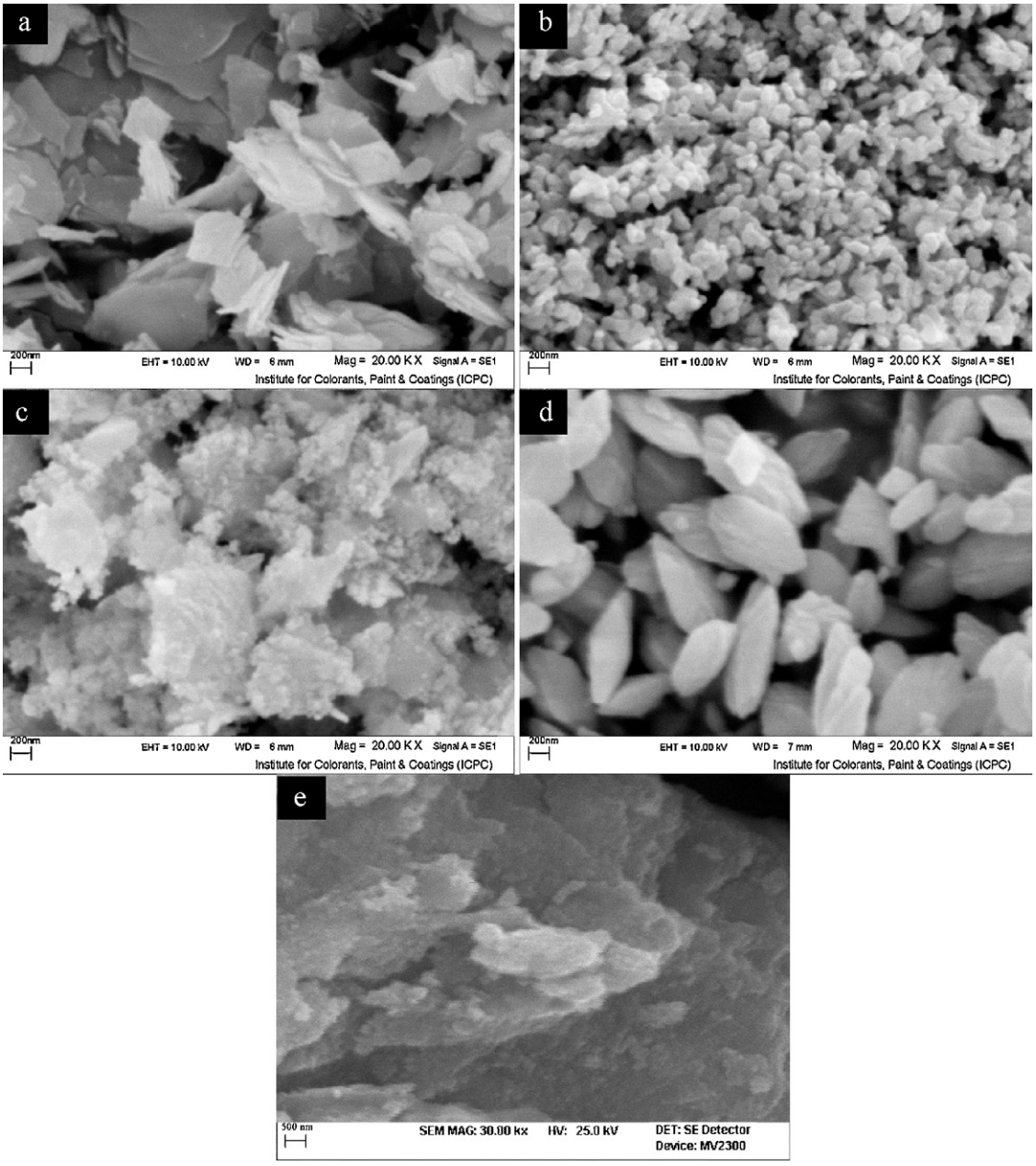

Fig. 9. SEM images of the $La_2(CO_3)_3$ nanoparticles: (a) sample no. 1, (b) sample no. 2, (c) sample no. 3, (d) sample no. 4, and (e) sample no. 13.

Table 2
Different approach for synthesis of lanthanum compounds nanostructures.

	Method	Materials	Product	Disadvantage	Ref. no.
1	Sol–gel	La_2O_3 PEG-20000 nitric acid	La_2O_3 nano particles	Long time 80 h, high temperature 800 °C	[20]
2	Reveres micelles or micro emulsion	Tx-100, cyclohexane, n-butylalcohol, Na_2CO_3 and $La(NO_3)_3{\cdot}xH_2O$	Nano wire of $La_2(CO_3)_3$	Much and expensive materials, long time 48 h	[21]
3	Hydrothermal	$La(NO_3)_3{\cdot}xH_2O$, citric acid and KOH	Nano spheres of $La(OH)_3$	Long time 12 h	[45]
4	Sol-solvothermal	$La(NO_3)_3{\cdot}xH_2O$, NH_3, benzene and n-butyl amine	Nano rod of $La(OH)_3$ and La_2O_3	Long time 12 h	[19]
5	Hydrothermal micro emulsion	CATB, cyclohexane, n-pentanol, $La(NO_3)_3{\cdot}xH_2O$ and KOH	Nano rod of $La(OH)_3$	Much and expensive materials, long time 12 h	[46]
6	Laser ablation	La_2O_3 and Fe_2O_3	Thin film of $LaFeO_3$	Expensive instruments	[22]
7	Wet chemical method	$La(NO_3)_3{\cdot}xH_2O$, N_2H_4, H_2O and NaOH	Nano rods of $La(OH)_3$	Long time 48 h	[23]
8	Micelless	$LaCl_3$, sodium dodecyl sulfate	La_2O_3 mesostructure	Long time 24 h	[47]
9	Solvothermal	1,1,3,3-Tetramethylguanidinium lactate (TMGL) and La_2O_3	$LaCO_3OH$ nanowires	Long time 48 h and need for expensive ionic liquid (TMGL)	[48]
10	Hydrothermal	Sodium linoleate, linoleate acid, $Ln(NO_3)_3$ (Ln = La, Ce, Pr, Nd, Sm, Eu, Gd, Th, Dy, Ho, Er, Tm, Yb, and Y) and NaF/or NH_4HF_2	Rare-earth fluoride nanocrystals	Need for heating 100–200 °C for about 8–10 h.	[49]
11	Solvothermal	Lanthanum nitrate ($La(NO_3)_3$), ethylene glycol monomethyl ether ($HO(CH_2)OCH_3$) and NaOH	Ultralong lanthanum hydroxide nanorods	Need for heating and long time (240 °C for 24 h)	[50]

tate at 600 °C, and no other absorption band was observed in the spectrum.

The energy dispersive spectrometry (EDS) analysis was employed to determine the composition of $La(OH)_3$ (sample no. 5), nanoparticles. As shown in Fig. 6, the EDS clearly identify that the nanoparticles are composed of O and La, with the molar ratio of about 3:1 (O/La), they should therefore be attributed to $La(OH)_3$, H cannot be detected by EDS, and further confirming the purity of products.

In addition, some other conditions were examined to investigate the morphology of products, if any, and compare them with each other. The relationship between the mean particle size of La_2O_3 and calcination temperature is plotted in Fig. 7 when the calcination time is 2 h. The result shows that the mean particle size increases with increasing calcination temperature. It grows slowly at lower temperature, and increases very quickly when the temperature is beyond 750 °C. Fig. 8a–d shows SEM images of the lanthanum oxide nanoparticles calcined at 650, 700, 750, and 800 °C for 2 h, respectively. Quasi-spherical nanoparticles are observed when the calcinations temperature is below 700 °C. At 750 °C, the particles have begun to agglomerate and grow up. When the temperature reaches to 800 °C, all particles have been sintered completely together leading to the formation of big particles [20]. The results reveal that the size of La_2O_3 nanoparticles depends on the calcination temperature. By increasing calcinations temperature, the larger La_2O_3 nanoparticles have been prepared.

For investigating the effect of sonication time on the morphology of the lanthanum carbonate, the reaction carried out in 15, 30, 45 and 60 min. As Fig. 9(a–d) shows with decreasing of aging time to 15 min (sample no. 1), the obtained particles were bigger than the particles of sample no. 2 with the aging time of 30 min. With increasing of the aging time to 45 and 60 min (samples no. 3 and 4) the nanoparticles with average size of 100 nm in diameter is produced. For investigation the effect of sonication for preparing of lanthanum carbonate, reaction was carried out without use of sonication (sample no. 13). Using sonication as procedure instead of co-precipitation gave smaller particles of lanthanum carbonate (compare Fig. 9e with b). Unlike the corresponding reaction via ultrasonic, in which a precipitate was observed immediately after sonication, by co-precipitation it took about 40 min for the white precipitate to appear. The obtained powder was characterized by XRD and FT-IR techniques (not shown here). The results were same as the presented figures for sample no. 2. For instance two significant absorption bands related to carbonate group were observed at 1504 cm^{-1} and 1426 cm^{-1} are attributed to the υ_3 mode of CO_3^{2-} group, but these absorption bands have a small shift respect to sample no. 2. According to the above results we can conclude that, the role of sonication in here is formation of nano-sized lanthanum carbonate compound. In two reactions (sample no. 2 and sample no. 13) water was used as solvent, without any surfactant and additive.

Fig. 10 shows the effect of surfactant on the morphology and the particle size of nanoparticles of lanthanum carbonate. From Fig. 10, it can be seen that in the presence of PEG as surfactant, sample no. 12, the surfactant hold the particles together so cause the formation of particles with morphology of scaly. So the surfactant is not necessary to be added for preparing lanthanum carbonate. It has been reported that the presence of capping molecule (such as PEG) can alter the surface energy of the crystallographic surface, and promote the anisotropic growth of nanocrystals and therefore we can see this trend in the case of lanthanum carbonate [42–44].

In comparison with to similar other works that is illustrated in Table 2, we used low cost, nontoxic precursor and solvent to synthesis $La_2(CO_3)_3$ nanoparticles by low cost, fast and simple sonochemical method. According to these results, by sonochemical method $La_2(CO_3)_3$ were prepared, then $La(OH)_3$ nanoparticles were prepared by hydrolysis of the obtained product and with calcinations of lanthanum carbonate at 600 °C for 2 h, the La_2O_3

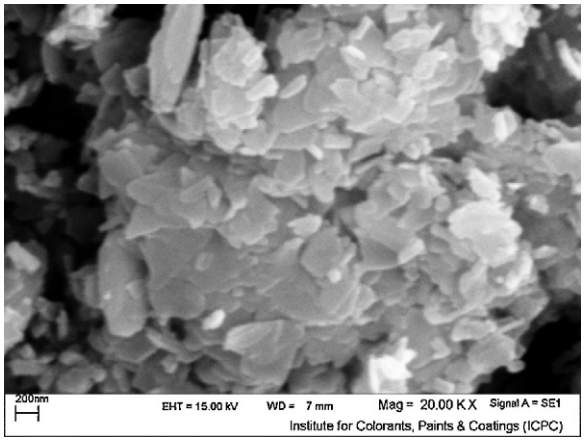

Fig. 10. SEM image of the lanthanum carbonate nanoparticles prepared in the presence of PEG (sample no. 12).

nanostructures as final product were synthesized successfully with the best conditions and smallest size.

4. Conclusion

In summary, novel $La_2(CO_3)_3{\cdot}1.7H_2O$ nanoparticles with the orthorhombic type were synthesized by a sonochemical method. This method brings forward a broad idea to synthesize other rare-earth compounds with various morphologies and novel properties. Lanthanum hydroxide with average size 20 nm were obtained from hydrolysis of $La_2(CO_3)_3{\cdot}xH_2O$ at 110 °C for 24 h. In summary, we have found a simple route to prepare La_2O_3 nanoparticles by facile thermal treatment of $La_2(CO_3)_3$. The XRD, TEM, SEM, XPS, and FTIR were used to characterize the products. The effect of some parameters such as time of sonication, calcinations temperature and addition of PEG as surfactant on the size and morphology of the obtained products were investigated. And we concluded that sonication time of 30 min and calcination temperature of 600 °C are optimum condition to synthesize lanthanum carbonate and lanthanum oxide, respectively and addition of surfactant is not necessary.

Acknowledgement

Authors are grateful to the council of University of Kashan for their unending effort to provide financial support to undertake this work.

References

[1] M.L. Lau, H.G. Jiang, R.J. Perez, J. Juarezislas, E.J. Lavernia, Nanostruct. Mater. 7 (1996) 847–856.
[2] M. Salavati-Niasari, F. Davar, Mater. Lett. 63 (2009) 441–443.
[3] M. Salavati-Niasari, F. Davar, M.R. Loghman-Estarki, J. Alloys Compd. 494 (2010) 199–204.
[4] F. Davar, Z. Fereshteh, M. Salavati-Niasari, J. Alloys Compd. 476 (2009) 797–801.
[5] M. Salavati-Niasari, D. Ghanbari, F. Davar, J. Alloys Compd. 488 (2009) 442–447.
[6] F. Kim, S. Connor, H. Song, P.D. Yang, Angew. Chem. Int. Ed. 43 (2004) 3673–3677.
[7] H. Zhang, D.R. Yang, D.S. Li, X.Y. Ma, D.L. Que, Cryst. Growth Des. 5 (2005) 547–550.
[8] H.T. Shi, L.M. Qi, J.M. Ma, H.M. Cheng, J. Am. Chem. Soc. 125 (2003) 3450–3451.
[9] A.H. Peruski, L.H. Johnson, L.F. Peruski, J. Immunol. Methods 263 (2005) 35–41.
[10] S.P. Fricker, Chem. Soc. Rev. 35 (2006) 524–533.
[11] P. Pisency, K. Husekova, K. Frohlich, J. Soltys, Mater. Sci. Semiconduc. Process. 7 (2004) 231–236.
[12] S. Vlange, A. Beauchaud, J. Barrault, Z. Gabelica, J. Catal. 251 (2007) 113–122.
[13] G.A.H. Mekhemer, B.A.A. Balboul, Colloids Surf. A: Physicochem. Eng. Asp. 181 (2001) 19–29.
[14] M.J. Escudero, X.R. Novoa, L. Daza, J. Power Sources 106 (2002) 196–205.
[15] J.Y. Li, H. Dai, X.H. Zhong, Y.F. Zhang, X.F. Ma, J. Meng, X.Q. Cao, J. Alloys Compd. 452 (2008) 406–409.
[16] J. Sun, X.P. Qiu, W.T. Zhu, Int. J. Hydrogen Energy 30 (2005) 437–445.
[17] S. Harke, H.D. Wiemhoöfer, W. Goöpel, Sens. Actuat.: B Chem. 1 (1990) 188–194.
[18] Y. Zhang, K. Han, T. Cheng, Z. Fang, Inorg. Chem. 46 (2007) 4713–4717.
[19] B. Tang, J. Ge, C. Wu, L. Zhuo, Z. Chen, Z. Shi, Y. Dong, Nanotechnology 15 (2004) 1273–1276.
[20] X. Wang, M. Wang, H. Song, B. Ding, Mater. Lett. 60 (2006) 2261–2265.
[21] G. Guo, F. Gu, Z. Wang, H. Guo, J. Crystal Growth 277 (2005) 631–635.
[22] M.F. Vignolo, S. Duhalde, M. Bormioli, G. Quintana, Appl. Surface Sci. 197 (2002) 522–526.
[23] J. Zhu, Z. Gui, Y. Ding, Mater. Lett. 62 (2008) 2373–2376.
[24] L.H. Qiu, V.G. Pol, J. Calderon Moreno, A. Gedanken, Ultrason. Sonochem. 12 (2005) 243–247.
[25] L. Zhu, X. Liu, Q. Li, S. Zhang, J. Meng, X. Cao, Nanotechnology 17 (2006) 4217–4222.
[26] J. Geng, J.J. Zhu, D.J. Lu, H.Y. Chen, Inorg. Chem. 45 (2006) 8403–8407.
[27] J. Geng, Y. Lv, D. Lu, J. Zhu, Nanotechnology 17 (2006) 2614–2620.
[28] K.S. Suslick, Ultrasound: It's Chemical, Physical and Biological Effects, VCH, Weinheim, Germany, 1988.
[29] K.S. Suslick, S.B. Choe, A.A. Cichowlas, M.W. Grinstaff, Nature 353 (1991) 414–416.
[30] P. Jeevanandam, Y. Koltypin, O. Palchik, A. Gedanken, J. Mater. Chem. 11 (2001) 869–873.
[31] J. Yang, C. Lin, Zh. Wang, J. Lin, Inorg. Chem. 45 (2006) 8973–8979.
[32] X. Ma, H. Zhang, Y. Ji, J. Xu, D. Yang, Mater. Lett. 58 (2004) 1180–1182.
[33] M. Zhou, J. Yuan, W. Yuan, Y. Yin, X. Hong, Nanotechnology 18 (2007) 405704–405710.
[34] M. Salavati-Niasari, F. Davar, Z. Fereshteh, J. Alloys Compd. 494 (2010) 410–414.
[35] M. Salavati-Niasari, F. Davar, M. Farhadi, J. Sol–Gel Sci. Technol. 51 (2009) 48–52.
[36] F. Mohandes, F. Davar, M. Salavati-Niasari, J. Magn. Magn. Mater. 322 (2010) 872–877.
[37] M. Salavati-Niasari, N. Mir, F. Davar, J. Alloys Compd. 476 (2009) 908–912.
[38] M. Salavati-Niasari, J. Javidi, F. Davar, Ultrason. Sonochem. 17 (2010) 870–877.
[39] A.I.Y. Tok, L.T. Su, F.Y.C. Boey, S.H. Ng, J. Nanosci. Nanotechnol. 7 (2007) 1–90.
[40] D.L. Zhao, Q. Yang, Z.H. Han, J. Zhou, S.B. Xu, F.Y. Sun, Solid State Sci. 10 (2008) 31–39.
[41] B. Klingenberg, M.A. Vannice, Chem. Mater. 8 (1996) 2755–2768.
[42] W.I. Park, D.H. Kim, S.W. Jung, G.C. Yi, Appl. Phys. Lett. 80 (2002) 4232–4234.
[43] X. Li, G. He, G. Xiao, H. Liu, M. Wang, J. Colloid Interface Sci. 333 (2009) 465–473.
[44] J. Du, Z. Liu, Y. Huang, Y. Gao, B. Han, W. Li, G. Yang, J. Cryst. Growth 280 (2005) 126–134.
[45] B. Tang, J. Ge, L. Zhuo, Nanotechnology 15 (2004) 1749–1751.
[46] Y.D. Yin, G.Y. Hong, Chin. Chem. Lett. 16 (2005) 1659–1662.
[47] J. Cao, H. Ji, J. Liu, M. Zheng, X. Chang, X. Ma, A. Zhang, Q. Xu, Mater. Lett. 59 (2005) 408–411.
[48] Z. Li, J. Zhang, J. Du, H. Gao, Y. Gao, T. Mu, B. Han, Mater. Lett. 59 (2005) 963–965.
[49] X. Wang, J. Zhuang, Q. Peng, Y. Li, Inorg. Chem. 45 (2006) 6661–6665.
[50] B. Hou, Y. Xu, D. Wu, Y. Sun, J Mater. Sci. 45 (2007) 1397–1400.